Continuum Mech. Thermodyn. (2019) 31:939–953
https://doi.org/10.1007/s00161-018-0653-7

ORIGINAL ARTICLE

A. P. S. Selvadurai

The Biot coefficient for a low permeability heterogeneous limestone

Received: 3 January 2018 / Accepted: 2 April 2018 / Published online: 12 April 2018

Abstract This paper presents the experimental and theoretical developments used to estimate the Biot coefficient for the heterogeneous Cobourg Limestone, which is characterized by its very low permeability. The coefficient forms an important component of the Biot poroelastic model that is used to examine coupled hydro-mechanical and thermo-hydro-mechanical processes in the fluid-saturated Cobourg Limestone. The constraints imposed by both the heterogeneous fabric and its extremely low intact permeability [$K \in (10^{-23}, 10^{-20})$ m^2] require the development of alternative approaches to estimate the Biot coefficient. Large specimen bench-scale triaxial tests (150 mm diameter and 300 mm long) that account for the scale of the heterogeneous fabric are complemented by results for the volume fraction-based mineralogical composition derived from XRD measurements. The compressibility of the solid phase is based on theoretical developments proposed in the mechanics of multi-phasic elastic materials. An appeal to the theory of multi-phasic elastic solids is the only feasible approach for examining the compressibility of the solid phase. The presence of a number of mineral species necessitates the use of the theories of Voigt, Reuss and Hill along with the theories proposed by Hashin and Shtrikman for developing bounds for the compressibility of the multi-phasic geologic material composing the skeletal fabric. The analytical estimates for the Biot coefficient for the Cobourg Limestone are compared with results for similar low permeability rocks reported in the literature.

Keywords Biot coefficient · Skeletal compressibility · Solid material compressibility · Voigt-Reuss-Hill estimates · Hashin-Rosen estimates · Cobourg limestone

1 Introduction

A proposed location for a Deep Geologic Repository (DGR) to store low- and intermediate-level radioactive waste is in the geologic formations at the Bruce Nuclear Facility on the eastern shores of Lake Huron in southern Ontario, Canada. This DGR will be located approximately 680 m below ground level within the Cobourg Limestone formation of the Paleozoic sedimentary sequence that rests on a Precambrian granitic gneiss basement rock. The Cobourg formation is overlain by upper Ordovician-age siltstone and grey shale extending to a thickness of approximately 200 m and underlain by argillaceous limestone and grey shale, approximately 150 m thick resting on the granitic basement rock. Despite its low clay content, the Cobourg Limestone is nominally referred to as an argillaceous limestone. A characteristic feature of the Cobourg Limestone is its heterogeneous fabric, consisting of lighter nodular regions of calcite and dolomite separated

Communicated by Francesco dell'Isola.

William Scott Professor and James McGill Professor.

A. P. S. Selvadurai (✉)
Department of Civil Engineering and Applied Mechanics, McGill University, Montréal, QC H3A 0C3, Canada
E-mail: patrick.selvadurai@mcgill.ca

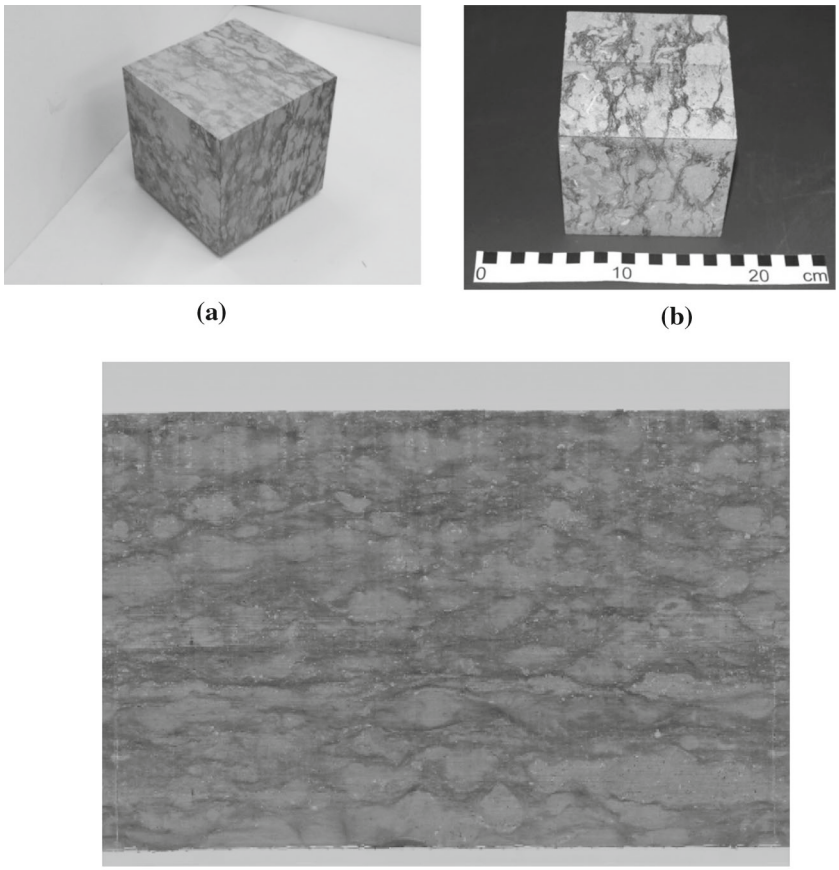

(a) **(b)**

(c)

Fig. 1 The heterogeneous Cobourg Limestone (**a**) heterogeneity in a 406 mm cube, (**b**) heterogeneity in a 130 mm cube, (**c**) panoramic view of the surface of 150 mm diameter cylinder

by argillaceous partings of a similar composition but with quartz and a low clay content (Fig. 1). The partings give the appearance of a distinct heterogeneity and nominal stratifications and raises important issues related to the representative volume elements that should be tested in order to obtain meaningful geomechanical properties relevant to the repository scale. X-ray tomographic imaging of small diameter (85 mm) samples of the Cobourg Limestone indicates that the heterogeneous fabric persists within the sample (Selvadurai [1]). The heterogeneity was also confirmed through the dissection of a large diameter cylinder measuring 150 mm in diameter and 300 mm in length.

The planned use of the Cobourg Limestone as the primary DGR setting requires the characterization of the poromechanical parameters that are important for defining coupled processes in the hydro-mechanical properties. In the event the argillaceous limestone formations are considered as repository locations for storing heat-emitting high-level nuclear waste; then it becomes necessary to also determine its thermo-hydro-mechanical properties. The theory of poroelasticity developed by Biot [2] represents a defining point in the mathematical modelling of coupled hydro-mechanical processes in fluid-saturated porous media. Although such theories have been developed in the context of soil mechanics (Terzaghi [3]), the theory proposed by Biot contains essential features that are relevant to the modelling of fluid-saturated rock masses. The theory has been extensively applied to problems involving geomechanical processes in fluid-saturated rocks (Coussy [4]; Selvadurai [5]; Cheng [6]; Selvadurai and Suvorov [7]) and has been extended to cover thermo-hydro-mechanical processes that are relevant to many geo-environmental processes encountered in deep geologic sequestration of heat-emitting nuclear fuel wastes (Selvadurai and Nguyen [8]; Selvadurai and Najari [9]), sequestration of CO_2 in fluidized forms, thermo-poroelastic processes resulting from glacial loading of sparsely fractured geologic formations (Selvadurai et al. [10]), heat generation during earthquake rupture and thermal stimulation of resource bearing formations for enhanced resource recovery (Selvadurai and Suvorov [7]). In its original

realm of application, Biot's theory of poroelasticity was developed to examine the mechanics of fluid-saturated geomaterials. The theory now has to its credit an extensive range of applications including in the modelling of bone material (Cowin [11]; Giorgio et al. [12]), nematic liquid crystals (Rosi et al. [13]) and in the modelling of fluid-saturated biomaterials including arterial tissue and brain material (Pence [14]; Selvadurai and Suvorov [15,16]; Suvorov and Selvadurai [17]).

An important aspect of Biot's theory of poroelasticity is the specification of the partitioning of externally applied stresses between the *porous skeleton* and the *pore fluid* saturating the pore space. The Biot formulation takes into consideration the compatibility of volumetric elastic deformations of the porous skeleton and that of the pore fluid. The theory of effective stress proposed by Terzaghi [3] has no observable connection to the notion of deformation compatibility between the pore fluid and the porous skeleton in the stress partitioning process. The pore pressure parameters proposed by Bruggeman et al. [18] and Skempton [19] follow the basic ideas proposed by Biot and extensions to other formulations that incorporate the compressibility of the solid material composing the porous skeleton are given by Bishop [20]. The estimation of Biot's coefficient for a very low permeability geologic medium with a heterogeneous porous fabric is not as straightforward as it is for soils and other high permeability rocks such as sandstone, limestone, porous tuff. The nature of the heterogeneity in terms of the spatial distribution of the various porous phases invariably requires a more precise definition of the effective elasticity properties of the solid material composing the porous fabric that are needed to evaluate the Biot coefficient.

2 The mineralogical and physical properties of the Cobourg Limestone

The Cobourg Limestone used in the research programme was obtained from an outcrop at the Saint Mary's Quarry in Bowmanville, Ontario. Extensive mechanical, physical and fluid transport investigations were performed by the research group and these are documented in the articles by Selvadurai et al. [21], Selvadurai and Jenner [22], Selvadurai and Najari [9,23], Selvadurai and Głowacki [24] and Selvadurai [1]. Of particular interest are the tests on cuboidal samples that were performed to establish the influence of sample size on the mass density and uniaxial compressive strength. Figure 2a shows the variation of mass density with the dimensions of the cuboid, and Fig. 2b shows the variation of the uniaxial compressive strength of the cuboidal specimens.

These results obtained indicate that the basic physical and mechanical properties show some dependency on the fabric heterogeneity of the Cobourg Limestone. The deformability characteristics in terms of the measured elastic modulus varied from 6.6 GPa (250 mm cube) to 17.7 GPa (200 mm cube) with an average of 13.5 GPa. These values are considerably lower than the Young's moduli estimated from triaxial tests on 85 mm diameter, 170 mm long cylindrical samples [1]. A separate test on a 250 mm cube with bonded strain gauges gave a Young's modulus of 35 GPa, consistent with the triaxial test data [1]. These preliminary results indicate that to eliminate the influence of heterogeneity on the basic geomechanical characterizations, the sample dimensions should be larger than 100 mm, which is approximately four times the size of the larger nodular regions. The XRT images of the 85 mm diameter and 170 mm long Cobourg Limestone cylinders lacked the RVE dimensions necessary to evaluate the relative volume fractions of the lighter grey nodular limestone and the darker argillaceous partings. These volume fractions were estimated using photographic images of thin slices (80 mm $\times$ 120 mm $\times$ 8 mm) obtained from a cuboidal prism [1]. A composite image of the spatial distribution of the lighter grey limestone is shown in Fig. 3. The volume fraction of the lighter grey limestone region was approximately 0.475, and that of the darker argillaceous partings was 0.525. To further investigate the volume fractions, a 150 mm diameter by 300 mm long cylinder was cut into 13 discs of nearly equal thickness. An image analysis of the photographs of both faces of each disc was then used to reconstruct the spatial distribution of the lighter and darker regions. These studies indicated that the area fraction of the darker grey argillaceous region exhibited wide variability, from 0.076 to 0.631, and the average area fraction of the darker argillaceous phase was approximately 0.36. The data obtained from the dissection of the cuboidal prism are considered more reliable due to the smaller thickness of the slabs used in the image analysis. In view of the variability in the estimation of the volume fraction of the darker argillaceous partings (V_{DR}), it is prudent to assign plausible limiting values to the parameter: i.e. $V_{\mathrm{DR}} \in (0.36,\ 0.53)$.

Two experimental procedures were used to estimate the mineralogical composition of the Cobourg Limestone. In the first procedure, XRF, XRD and JEOL electron probe analyses were used to estimate the mineralogical composition of samples recovered from powder, fragments and discs. For the powder samples, visible light and dark grey species were etched from the surface of large Cobourg Limestone cubes with a hardened

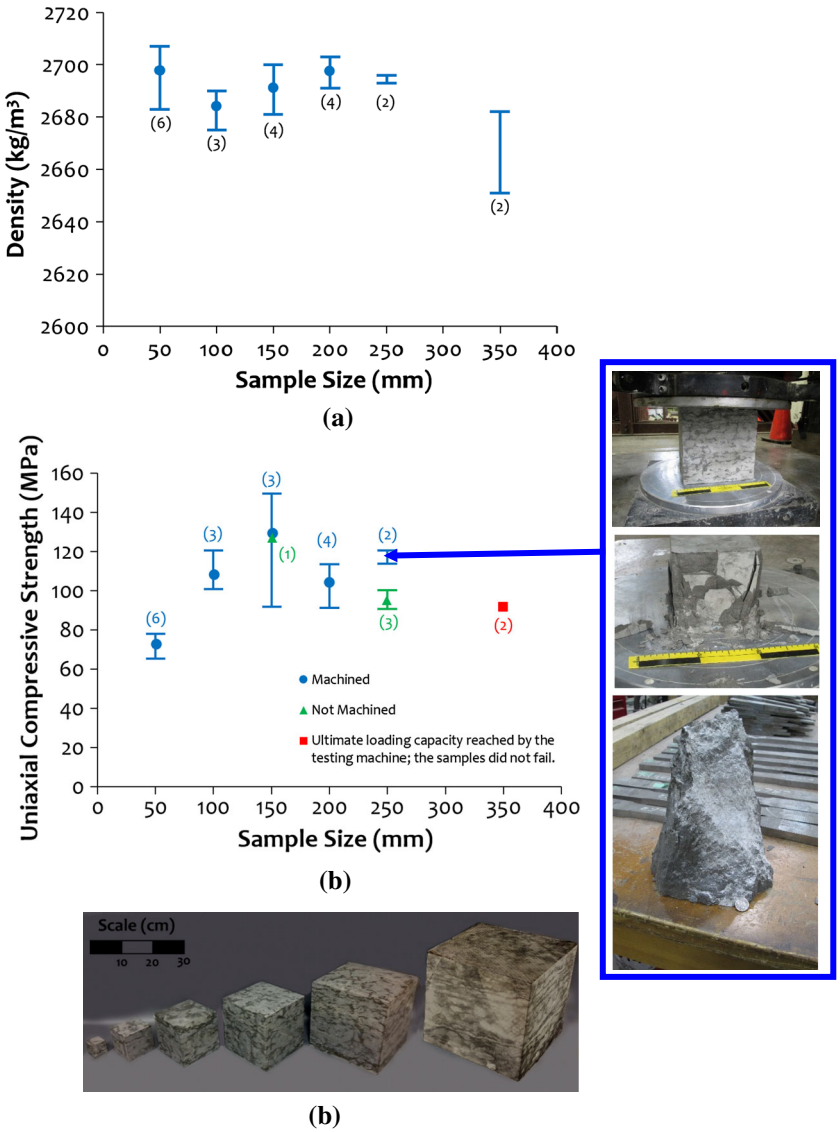

Fig. 2 Size dependency in the Cobourg Limestone. (**a**) Variation of density and (**b**) variation of uniaxial compressive strength with sample size

steel hook to collect approximately 1 g of the material. For the fragmented samples, light and dark grey regions were selected and hit with a hammer to delaminate the particular species. The disc sections were cut from 25 mm diameter core samples at selected areas of a particular species; these sections were machined on a lathe to obtain a disc (2–3 mm in thickness and 25 mm in diameter), which allowed it to be analysed in the XRD apparatus. Table 1 shows the relative mineralogical composition of the lighter and darker phases of the Cobourg Limestone. In the second approach the mineralogical compositions were determined using a EDS Probe incorporated on a Zeiss Sigma-Gemini SEM apparatus. The mineralogical compositions obtained by averaging results of both experimental procedures are given below, and the bulk modulus of the minerals is also indicated:

(i) The Lighter Grey Nodular Phase
Calcite ∼ 86%; Dolomite ∼ 5%; Quartz ∼ 8%; Clay ∼ 0.3%;
Porosity ∼ 0.001

(ii) The Darker Argillaceous Partings
Calcite ∼ 51%; Dolomite ∼ 16%; Quartz ∼ 22%; Clay ∼ 2.4%;
Porosity ∼ 0.006

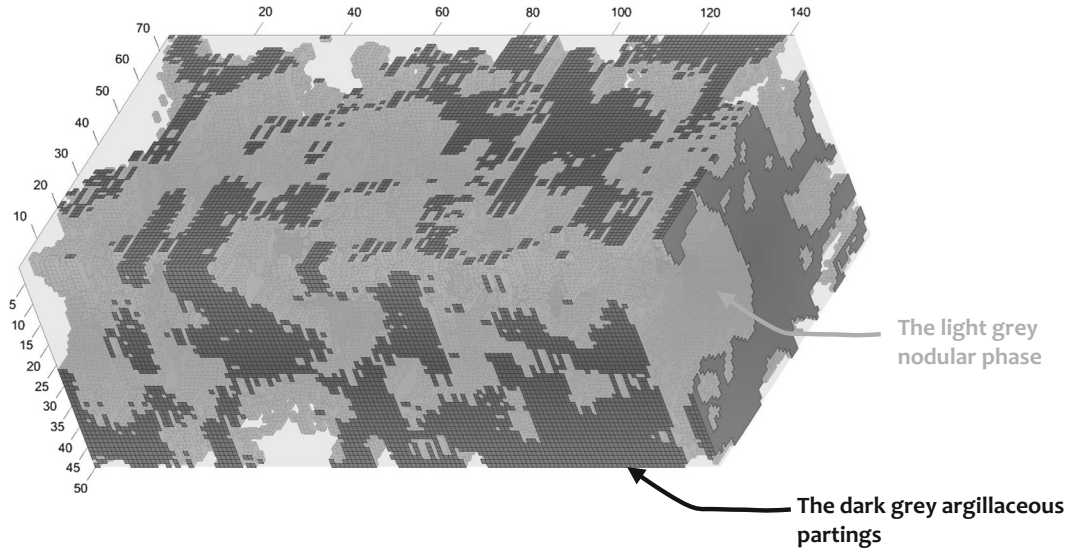

Fig. 3 The spatial distribution of the lighter and darker phases of the Cobourg Limestone, derived from an assembly of images obtained from sectioning a cuboidal sample

Table 1 Mineralogical composition of the Cobourg Limestone

Light grey		Dark grey	
Minerals	%	Minerals	Variance %
Quartz	8.01	Quartz	22.00 ± 5.9
Calcite	85.4	Calcite	51.45 ± 13.3
Dolomite	5.3	Dolomite	15.85 ± 6.6
Albite	0.73	Albite	3.25 ± 1.1
Microcline	0.25	Microcline	3.00 ± 0.2
Muscovite	0.16	Muscovite	1.55 ± 0.9
Chlorite	0.13	Chlorite	0.80 ± 0.3
Pyrite	0.08	Pyrite	1.45 ± 0.8
Haematite	0.03	Haematite	0.65 ± 0.2

(iii) Bulk Modulus and Shear Modulus Values

The values for the bulk moduli $(K_S)_i$ and shear moduli $(G_S)_i (i$ = Calc, Dolm, Qrtz, Clay) of the basic minerals constituting the Cobourg Limestone can be obtained from published literature (Carmichael [25]; Berge and Berryman [26]; Redfern and Angel [27]; Vanorio et al. [28]; Lin [29])

Calcite: $(K_S)_{\text{Calc}} = 76$ GPa; $(G_S)_{\text{Calc}} = 32$ GPa

Dolomite: $(K_S)_{\text{Dolm}} = 95$ GPa; $(G_S)_{\text{Dolm}} = 45$ GPa

Quartz: $(K_S)_{\text{Qrtz}} = 37$ GPa; $(G_S)_{\text{Qrtz}} = 45$ GPa

Clay: $(K_S)_{\text{Clay}} = 12$ GPa; $(G_S)_{\text{Clay}} = 6$ GPa

There is reasonable similarity between the results for the mineralogical composition derived from the two procedures. The above set of values will be used to estimate the effective bulk modulus of the solid material constituting the porous skeleton. The porosity of the lighter and darker phases was determined using Mercury Intrusion Porosimetry (MIP). The results are slightly lower than the bulk values observed in previous investigations: Vilks and Miller [30] ~ 0.017, Selvadurai et al. [21] ~ 0.015, Selvadurai and Jenner [22] ~ 0.01, Selvadurai and Najari [23,31] ~ 0.006 to 0.04, Selvadurai and Głowacki [24] ~ 0.01. SEM images of the Cobourg Limestone indicate a clear demarcation boundary between the light grey calcite-dolomite regions and the dark grey calcite-dolomite regions with a clay fraction (Fig. 4). The spatial variation of physical parameters such as porosity, however, cannot be readily estimated without appeal to micromechanical testing.

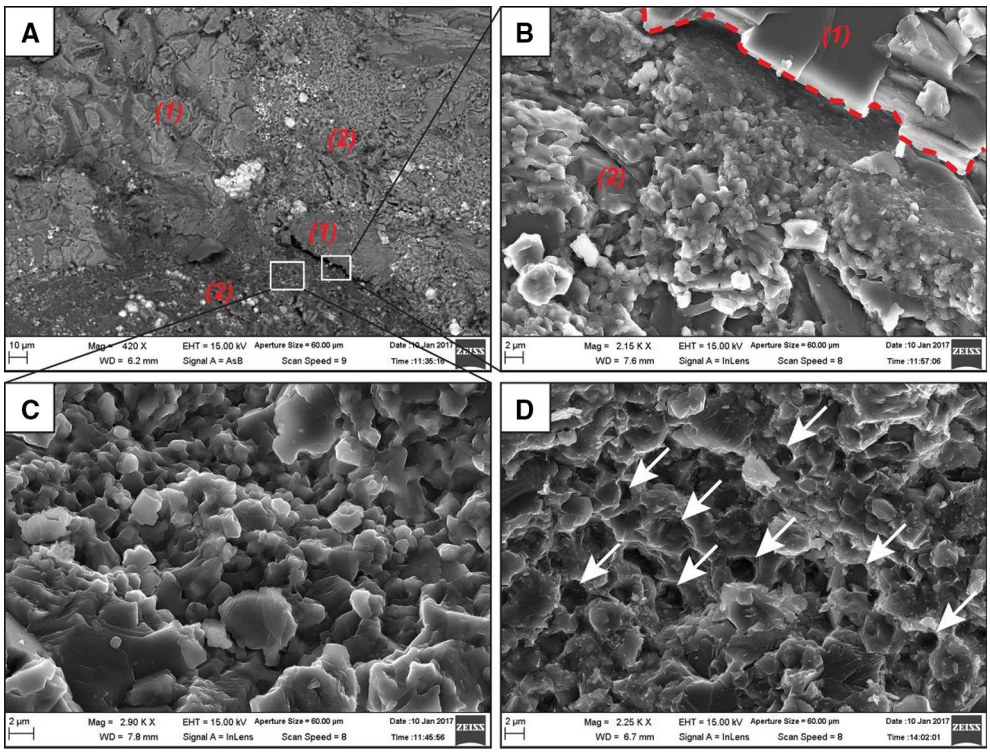

Fig. 4 **a** A SEM image of the Cobourg Limestone composition with boundary between the two micro-texture phases: (1) the main calcite phase and (2) the argillaceous phase, **b** close-up of the micro-texture boundary of picture **a**, **c** matrix layout of the argillaceous area, **d** well-developed micro-porosity network in the argillaceous part

3 Triaxial testing of a dry Cobourg Limestone cylinder

The skeletal compressibility characteristics of the Cobourg Limestone were determined by testing a 150 mm diameter and 300 mm long cylinder, which was oven-dried at 70°C for one week. The cylinder was weighed periodically to ensure that the absorbed moisture was removed during the drying process.

The large sample needed to capture a representative volume required the use of a large triaxial cell specially designed and built by GDS Instruments. The schematic arrangements of the GDS Active Triaxial Cell are shown in Fig. 5, and the schematic view of the experimental facilities for conducting triaxial tests is given in Fig. 6. The application of cell pressures and axial loads to the Cobourg Limestone cylinder is controlled through two 64 MPa GDS pressure controllers as shown in Fig. 6. The plane ends of the Cobourg Limestone cylinder were machined to a parallel finish and were in direct contact with the loading platens (Fig. 5). The axial deformations of the cylinder during the application of either the cell pressure or the deviatoric stresses were monitored with a specially designed harness containing 3 LVDTs connected to the loading platens. The cell pressure, the axial load and LVDT data were collected continuously through a 16-bit data logger.

The GDS Active Triaxial Cell and test facility were used to determine the skeletal elasticity properties of the oven-dried large diameter Cobourg Limestone cylinder. Initially, the test specimen was subjected to increasing cell pressure and, upon attainment of a linear range in the isotropic stress with the axial strain, the cell pressure was maintained at a constant value, and the deviator stresses were applied. During both loading excursions, the axial strain in the Cobourg cylinder was measured. A typical experimental result is shown in black in Fig. 7. The experiment was repeated, and except for a shift in the origin of the test (the red curve in Fig. 6), the experimental results were remarkably similar. The shift in the origin can be corrected, but this is unnecessary since the elasticity properties relevant to the skeletal behaviour are determined by considering the slopes of the linear range of the loading curves (points A, B and C in Fig. 6). Additional uniaxial compression tests were performed on a separate 150 mm diameter and 300 long sample of the Cobourg Limestone to determine the skeletal elastic modulus, which was estimated to be between 34 and 36 GPa.

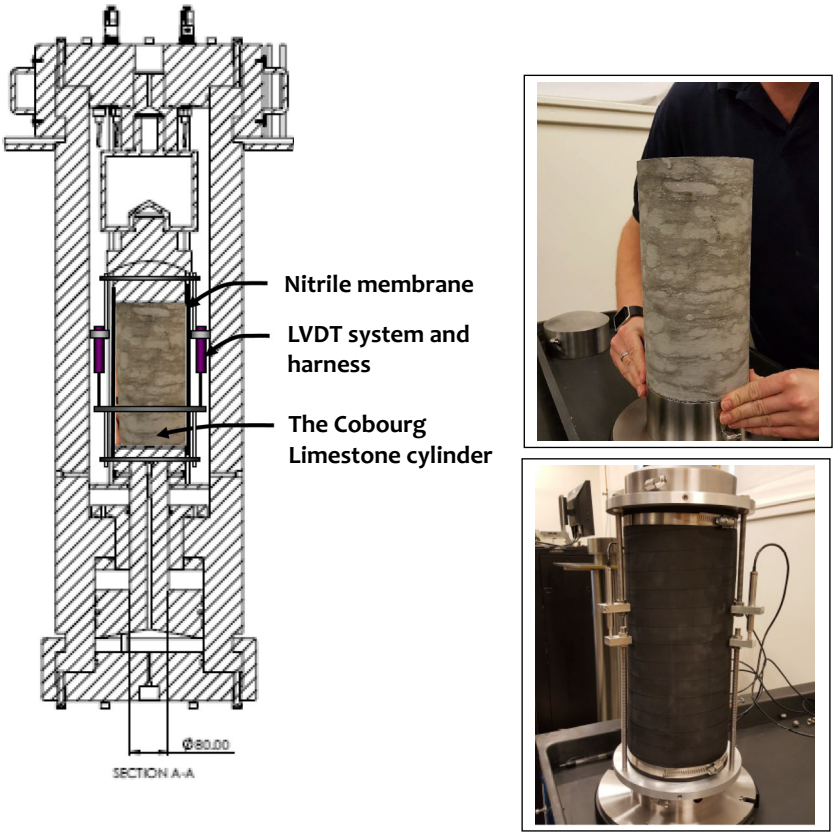

Fig. 5 The GDS Active Triaxial Cell for testing the Cobourg Limestone cylinder, measuring 150 mm in diameter and 300 mm in length and the LVDT arrangement

4 Theoretical approaches for the estimation of the Biot coefficient

In principle, estimating the Biot coefficient for a geomaterial is quite straightforward and requires only the estimation of the *bulk modulus of the porous skeleton* and the *effective bulk modulus of the solid phase constituting the porous skeleton*. The effective stress principle proposed by Biot [2] takes the form

$$\sigma_{ij} = \sigma'_{ij} + \alpha p \delta_{ij} \tag{1}$$

In (1), σ_{ij} is the total stress, σ'_{ij} is the effective stress, δ_{ij} is Kronecker's delta function and α is the "Biot Coefficient", defined by

$$\alpha = 1 - \frac{K_D}{K_S} \tag{2}$$

where K_D is the bulk modulus of the porous skeleton and K_S is the bulk modulus of the material composing the porous skeleton. If the bulk modulus of the porous skeleton is much smaller than the effective bulk modulus of the material, i.e. $(K_D/K_S) \ll 1$, then Biot's result converges to the result by Terzaghi [3].

In an experiment, the bulk modulus of the porous skeleton corresponds to the bulk modulus of the material in an air-dried or oven-dried condition, ensuring that there is no material damage during the removal of any moisture from the pore space. Schematically, the stages in the determination of K_D and K_S are illustrated in Fig. 8. In the first example (Fig. 8a), the pore space of the rock is dry and the sample is subjected to isotropic compression. The volumetric strain of the sample obtained from such a test can be used to estimate K_D. In the second example, illustrated in Fig. 8b, a fully saturated and jacketed sample of the rock is subjected to isotropic compression and the pore fluid pressures in the sample are allowed to attain equilibrium with the externally applied isotropic compression. The volumetric strain experienced by the sample during this test will correspond to the *volumetric strain of the skeletal material*, which can be used to estimate the value of K_S. The former test is straightforward but the latter test to estimate the value of K_S can be influenced by the permeability of

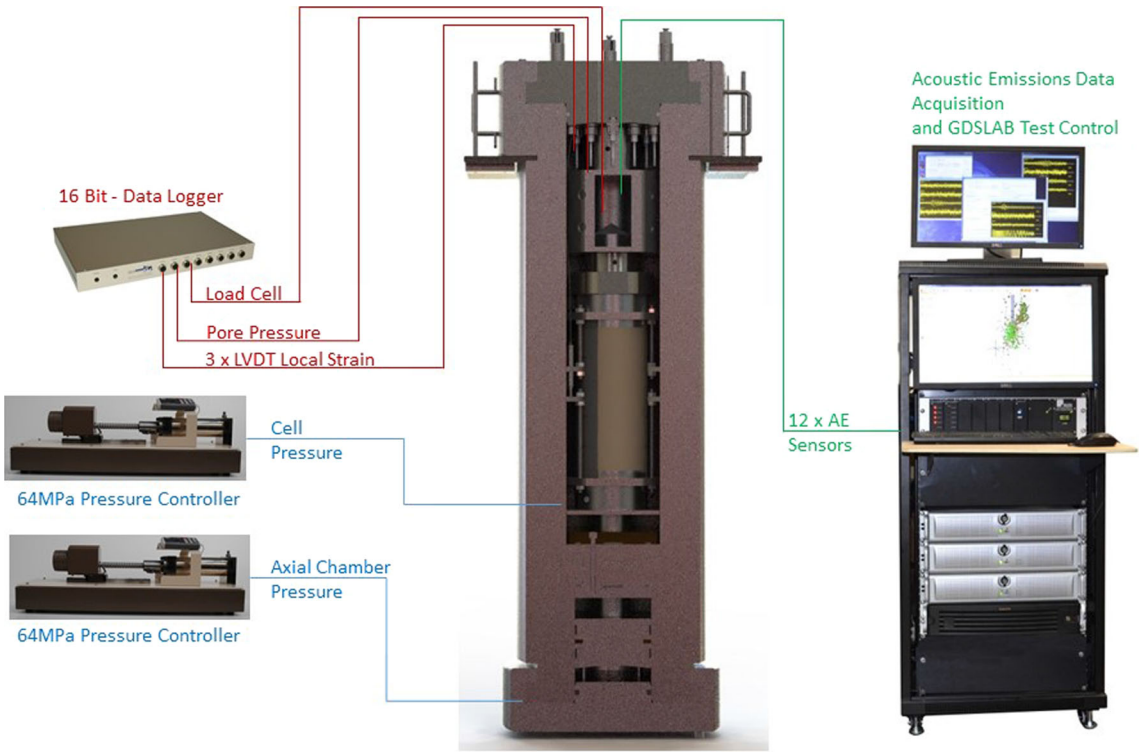

Fig. 6 A schematic view of the GDS Active Triaxial Cell testing facility

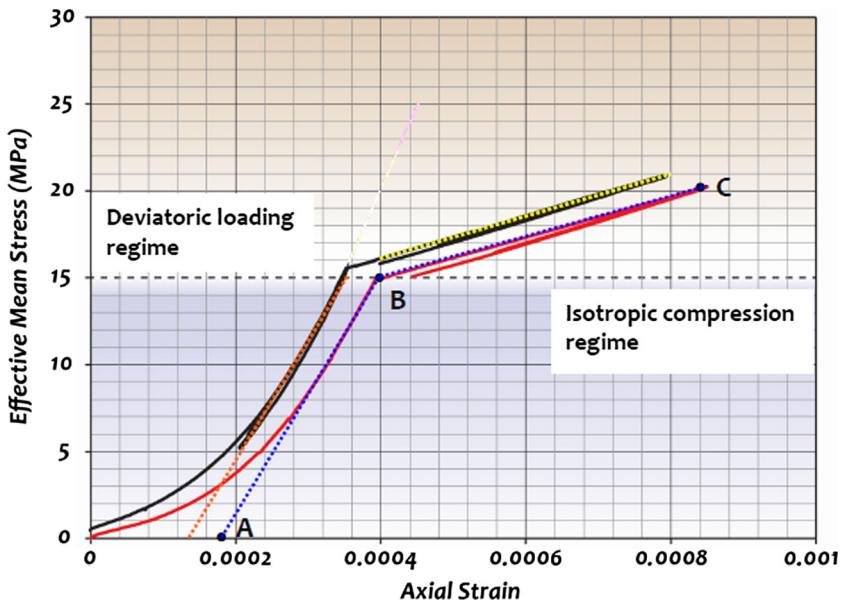

Fig. 7 Experimental results from the GDS Active Triaxial Cell testing facility

the porous medium. The above procedure has been successfully applied to estimate the Biot coefficient for a variety of rock including sandstone, granite, limestone, and examples of the results derived from experiments are documented in articles and volumes by Detournay and Cheng [32], Wang [33], Coussy [4], Lion et al. [34], Cheng [6], Wang et al. [35] and Armand et al. [36].

For a low permeability porous medium such as the Cobourg Limestone, additional time will be required for the pore water to reach fluid pressures equal to those applied at the boundary of the sample. It should be noted

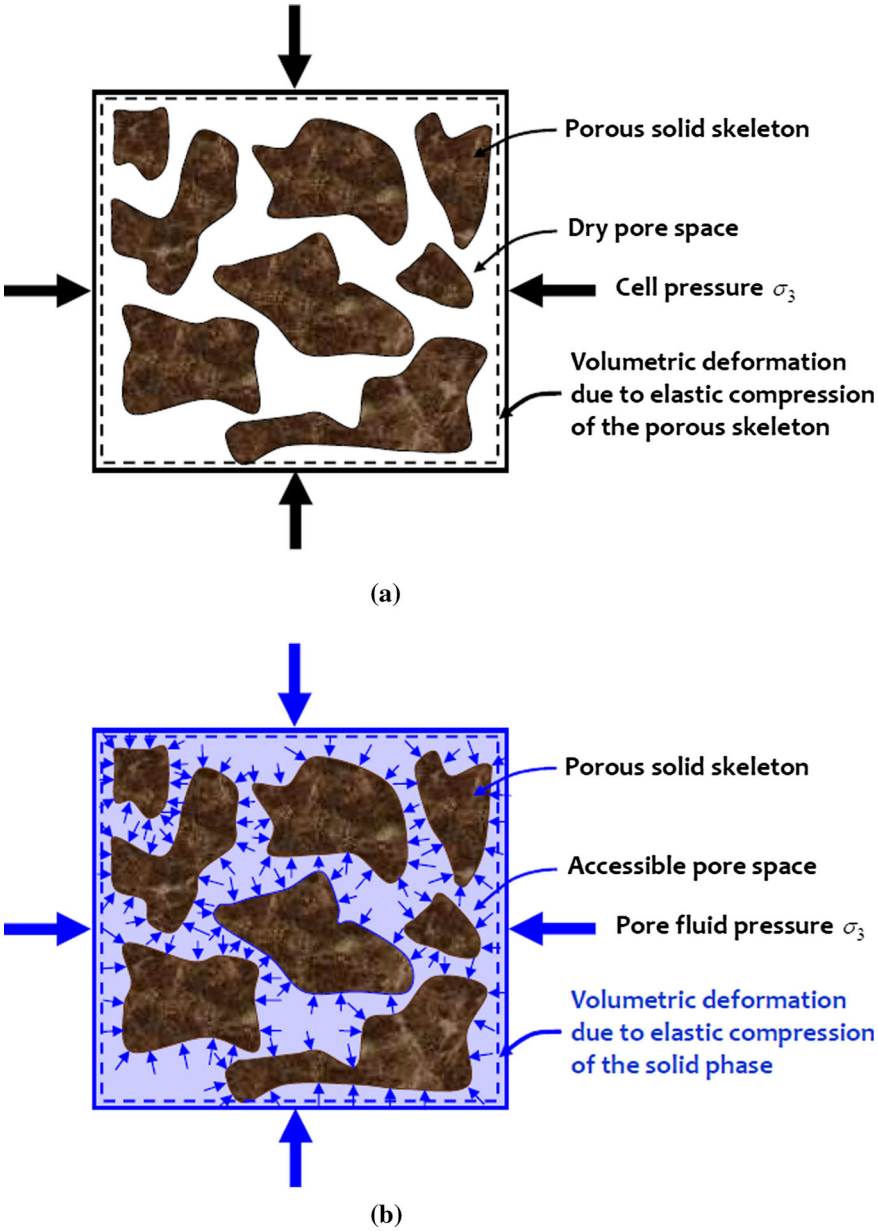

Fig. 8 Schematic representation of experiments required for estimating the Biot constant. **a** Test for estimating K_D, **b** test for estimating K_S

that there is no strict definition of what constitutes a low permeability geomaterial. The experimental results presented in [21–24,30,31,37] identify a range of geomaterials, both natural and constructed, that could be designated as having low permeability. For the Cobourg Limestone, with porosities ranging from 0.5 to 4%, the permeabilities can range from 10^{-22} to 10^{-19} m^2. Since the shortest flow path in the cylinder will correspond to the radial direction of the cylinder, the problem can be formulated as a radially symmetric problem in the theory of poroelasticity, where the pore fluid pressure at the boundary of the cylinder will correspond to the applied pressure p_0, and the radial effective or skeletal stresses are zero. As a simple illustration of this time requirement, we can consider the simpler radially symmetric problem of the time-dependent development of pressure in a circular porous medium, which is governed by the diffusion equation

$$\alpha^2 \left(\frac{\partial^2 p}{\partial r^2} + \frac{1}{r} \frac{\partial p}{\partial r} \right) = \frac{\partial p}{\partial t} \tag{3}$$

where

$$\alpha^2 = \frac{K}{\eta_f (n C_f + C_D)} \tag{4}$$

and K is the permeability of the porous medium, η_f is the dynamic viscosity of the fluid, n is the porosity, and C_f and C_D are, respectively, the compressibilities of the fluid and the porous skeleton (Selvadurai [38]). Other factors such as the compressibility of the solid material constituting the porous fabric can be included in (4), but this will not greatly influence the results since the compressibility of the solid phase is orders of magnitude lower than the skeletal compressibility. Initially, the pore pressure in the circular domain is zero, and at time $t = 0$, the boundary of the circular region is subjected to a pressure pulse. The pore pressure diffusion into a circular region of radius a is governed by the following boundary condition and initial condition:

$$p(a, t) = p_0 \mathrm{H}(t); \quad \forall t \geq 0 \tag{5}$$

$$p(r, 0) = 0; \quad 0 \leq r \leq a \tag{6}$$

where $\mathrm{H}(t)$ is the Heaviside step function of time. In addition, the pore pressures with the region should be finite at all times. The pore pressure diffusion problem can be solved either in relation to the analogous heat conduction problem (Carslaw and Jaeger [39]) or the chemical diffusion problem. Avoiding details, the solution to the pressure development in the circular porous region can be obtained [38] as

$$p(r, t) = p_0 \left(1 - 2 \sum_{n=1,2,}^{\infty} \frac{\exp\left(-k_n^2 \alpha^2 t\right) J_0(k_n r)}{[k_n a J_1(k_n a)]} \right) \tag{7}$$

where J_0 and J_1 are, respectively, zeroth-order and first-order Bessel functions of the first kind and k_n are the roots of the characteristic equation

$$J_0(ka) = 0 \tag{8}$$

We can focus attention on the development of pore fluid pressures at the centre of the circular region, which is given by

$$p(0, t) = p_0 \left(1 - 2 \sum_{n=1,2,}^{\infty} \frac{\exp\left(-k_n^2 \alpha^2 t\right)}{[k_n a J_1(k_n a)]} \right) \tag{9}$$

Considering typical values applicable to the low permeability Cobourg Limestone and the experimental configuration:

$$\begin{aligned} &K = 10^{-23}\ \mathrm{m}^2; \quad C_D = 4 \times 10^{-11}\ (\mathrm{Pa})^{-1}; \quad C_f = 4.35 \times 10^{-10}\ (\mathrm{Pa})^{-1} \\ &n = 0.006; \quad a = 0.075\ \mathrm{m}; \quad \eta_f = 0.001\ \mathrm{Pa\ s} \end{aligned} \tag{10}$$

we can evaluate (9) to ascertain the time–dependent rise in the pore fluid pressure at the centre of the circular region; for the experimental configuration indicated by (10), it will take approximately 167 days for the pore water pressure at the centre of the circular region to reach 95% of the pressure applied at the boundary. This value will vary with the permeability of the medium; an increase of K to 10^{-22} m^2 will require about 17 days to attain the 95% value. More time will be needed to reach saturation if the pore space contains undissolved air, which can increase the effective fluid compressibility. The problem can also be examined using a Biot [2] poroelasticity formulation but the results are particularly sensitive to the fluid compressibility. For example, computational results using the ABAQUS code indicate that if the fluid compressibility is an order of magnitude larger (i.e. $C_f = 4.35 \times 10^{-9}\ (\mathrm{Pa})^{-1}$), the time required for the pressure at the centre to attain 95% of the boundary pressure is approximately 178 days. Similarly, if the fluid compressibility is $C_f = 4.35 \times 10^{-8}\ (\mathrm{Pa})^{-1}$, the time required for the pressure at the centre to reach 95% of the boundary pressure is approximately 1112 days. This places a restriction on the reliability of the conventional approach for estimating K_S through the pressurization of a fully saturated sample of a low permeability rock. Furthermore, the laboratory techniques used to saturate a low permeability rock cannot guarantee complete saturation of all the accessible pore space. (In a field setting, however, geological time, stress states and fluid supply can result is saturated conditions, despite the low permeability characteristics of the rock.) Furthermore, if pressures are applied to induce saturation, sufficient time should elapse for dissipation of residual pressures that can influence the subsequent deformation response of the rock [40]. For this reason, alternative procedures developed for the study of multi-phasic elastic materials should be used to develop an estimate for K_S.

The elasticity properties of multi-phasic materials can be determined using a range of theoretical estimates that have been developed in the literature (Voigt [41]; Reuss [42]; Hill [43,44]; Hashin and Shtrikman [45]) and accounts of advances in this area are given, among others, by Hashin [46], Walpole [47], Hale [48], Christensen [49], Francfort and Murat [50], Sisodia and Verma [51], Ju and Chen [52,53], Nemat-Nasser and Hori [54], Torquato et al. [55], Lin and Ju [56], Suvorov and Selvadurai [57]. The volumes by Avseth et al. [58] and Mavko et al. [59] present compilations of applications of these developments to the study of rock properties. While the models available have wide ranging applications, the simplest estimates that have found applications to the study of effective elasticity properties of rocks relate to the bounds for the bulk moduli developed by Hashin and Shtrikman [45]. The procedure adopted here will regard the lighter grey nodular component of the Cobourg Limestone as one phase (*subscript* $(\,)_{\mathrm{LR}}$) and the darker grey argillaceous partings as a second phase (*subscript* $(\,)_{\mathrm{DR}}$). It is also noted that the lighter and darker regions are themselves composed of several mineral phases, consisting of calcite, dolomite, quartz, clay and voids of varying proportions. Therefore, in order the determine the effective bulk moduli of the solid phase of the Cobourg Limestone, it is necessary to determine the bulk moduli of both the lighter and darker phases of the Cobourg Limestone, which entails the use of a theory capable of estimating the effective bulk modulus of a multi-phasic elastic material composed of four separate solid phases. To the author's knowledge, there are no known theoretical formulations that can be used to assess the effective compressibilities of a four-component multi-phasic material, other than the basic estimates of Voigt and Reuss. The work of Hill [43] suggests a simpler algebraic average as an estimate that can be used to narrow down the wide range that can be encountered when using the Voigt and Reuss estimates separately.

The Voigt–Reuss–Hill estimate for the lighter grey $[(\,)_{\mathrm{LR}}]$ and the darker argillaceous $[(\,)_{\mathrm{DR}}]$ phases can be written as

$$(K_S)_I = \frac{1}{2}\left\{\sum_i^n V_i (K_S)_i + \left(\sum_i^n \frac{V_i}{(K_S)_i}\right)^{-1}\right\}; \quad I = \mathrm{LR,DR}; \quad i = \mathrm{Calc, Dolm, Qrtz, Clay, Voids} \tag{11}$$

and V_i are the separate volume fractions. We further postulate that the Voigt–Reuss–Hill estimate for the shear modulus of the lighter grey $[(\,)_{\mathrm{LR}}]$ and the darker argillaceous $[(\,)_{\mathrm{DR}}]$ phases can be written as

$$(G_S)_I = \frac{1}{2}\left\{\sum_i^n V_i (G_S)_i + \left(\sum_i^n \frac{V_i}{(G_S)_i}\right)^{-1}\right\}; \quad I = \mathrm{LR,DR}; \quad i = \mathrm{Calc, Dolm, Qrtz, Clay, Voids} \tag{12}$$

These estimates can now be used, in conjunction with the bounds developed by Hashin and Shtrikman [45], to estimate the *upper* and *lower* composite bulk moduli for K_S of the solid material of the Cobourg Limestone. Since the lighter phase has a higher fraction of dolomite, it is likely to yield the lower bound estimate. Assuming that the darker argillaceous phase, $[(\,)_{\mathrm{DR}}]$, with higher percentages of *dolomite* and quartz, yields the upper bound estimate, the lower and upper bounds for the effective compressibility of the solid material of the Cobourg Limestone, denoted respectively by $(K_S)_L$ and $(K_S)_U$, can be obtained from the results

$$(K_S)_L = (K_S)_{\mathrm{LR}} + \frac{V_{\mathrm{DR}}}{\frac{1}{(K_S)_{\mathrm{DR}} - (K_S)_{\mathrm{LR}}} + \left(\frac{3(1-V_{\mathrm{DR}})}{3(K_S)_{\mathrm{LR}} + 4(G_S)_{\mathrm{LR}}}\right)} \tag{13}$$

and

$$(K_S)_U = (K_S)_{\mathrm{DR}} + \frac{1 - V_{\mathrm{DR}}}{\frac{1}{(K_S)_{\mathrm{LR}} - (K_S)_{\mathrm{DR}}} + \left(\frac{3V_{\mathrm{DR}}}{3(K_S)_{\mathrm{DR}} + 4(G_S)_{\mathrm{DR}}}\right)} \tag{14}$$

These bounds converge to the proper limits as $V_{\mathrm{DR}} \to 1$ and $V_{\mathrm{DR}} \to 0$. For purposes of future reference, the *upper* and *lower* bounds for the shear modulus of the solid phase in the Cobourg Limestone can be estimated from the expressions

$$(G_S)_L = (G_S)_{\mathrm{LR}} + \frac{V_{\mathrm{DR}}}{\frac{1}{(G_S)_{\mathrm{DR}} - (G_S)_{\mathrm{LR}}} + \left(\frac{6(1-V_{\mathrm{DR}})[(K_S)_{\mathrm{LR}} + 2(G_S)_{\mathrm{LR}}]}{5(G_S)_{\mathrm{LR}}[3(K_S)_{\mathrm{LR}} + 4(G_S)_{\mathrm{LR}}]}\right)} \tag{15}$$

and

$$(G_S)_U = (G_S)_{\mathrm{DR}} + \frac{1 - V_{\mathrm{DR}}}{\frac{1}{(G_S)_{\mathrm{LR}} - (G_S)_{\mathrm{DR}}} + \left(\frac{6V_{\mathrm{DR}}[(K_S)_{\mathrm{DR}} + 2(G_S)_{\mathrm{DR}}]}{5(G_S)_{\mathrm{DR}}[3(K_S)_{\mathrm{DR}} + 4(G_S)_{\mathrm{DR}}]}\right)}, \tag{16}$$

respectively.

5 Numerical results

Typical triaxial test results from the large diameter Cobourg Limestone specimen are shown in Fig. 7. The initial linear elastic response, indicated by the slope AB, can be used to estimate the skeletal bulk modulus K_D. Assuming isotropic elastic behaviour of the skeletal response, the skeletal elastic bulk modulus can be obtained from

$$K_D = \frac{(\sigma_{zz})^B - (\sigma_{zz})^A}{3\left[(\varepsilon_{zz})^B - (\varepsilon_{zz})^A\right]} \tag{17}$$

Similarly, considering the isotropic elastic behaviour of the Cobourg during application of both cell pressure and deviatoric stress, indicated by BC in Fig. 7, the skeletal elastic modulus E_D can be obtained from

$$E_D = \frac{(\sigma_{zz})^C\left[(\sigma_{rr})^B + (\sigma_{\theta\theta})^B\right] - (\sigma_{zz})^B\left[(\sigma_{rr})^C + (\sigma_{\theta\theta})^C\right]}{(\varepsilon_{zz})^C\left[(\sigma_{rr})^B + (\sigma_{\theta\theta})^B\right] - (\varepsilon_{zz})^B\left[(\sigma_{rr})^C + (\sigma_{\theta\theta})^C\right]} \tag{18}$$

Noting that (i) at the stress state B, $(\sigma_{rr})^B = (\sigma_{\theta\theta})^B = (\sigma_{zz})^B = 15$ MPa, $(\varepsilon_{zz})^A \approx 0.00018$, and $(\varepsilon_{zz})^B \approx 0.0004$, and (ii) at the stress state C, $(\sigma_{rr})^C = (\sigma_{\theta\theta})^C = 15$ MPa, $(\sigma_{zz})^C = 30$ MPa and $(\varepsilon_{zz})^C \approx 0.00084$, we obtain

$$K_D \approx 22.73 \text{ GPa}; \quad E_D \approx 34.09 \text{ GPa}; \quad \nu_D \approx 0.25; \quad G_D \approx 13.63 \text{ GPa} \tag{19}$$

From (11) and (12) and the properties of the constituent phases, we obtain

$$(K_S)_{\text{LR}} \approx 71.63 \text{ GPa}; \quad (G_S)_{\text{LR}} \approx 33.22 \text{ GPa}$$
$$(K_S)_{\text{DR}} \approx 61.79 \text{ GPa}; \quad (G_S)_{\text{DR}} \approx 34.40 \text{ GPa}$$

which can be used in (13) and (14), with $V_{\text{DR}} \in (0.36, 0.53)$ to arrive at upper and lower bound estimates for the compressibility of the solid phase of the Cobourg Limestone. Considering the lower estimate for $V_{\text{DR}} = 0.36$, we obtain

$$67.88 \text{ GPa} \leq (K_S) \leq 67.89 \text{ GPa} \tag{20}$$

For the upper estimate of $V_{\text{DR}} = 0.53$, we obtain

$$66.00 \text{ GPa} \leq (K_S) \leq 66.20 \text{ GPa} \tag{21}$$

The estimated bounds for K_S do not display a strong dependency in the range of volume fractions assigned for V_{DR}. For subsequent estimations of the Biot coefficient, we assume that

$$66.00 \text{ GPa} \leq (K_S) \leq 67.89 \text{ GPa}. \tag{22}$$

Using (2), (19) and (22), the bounds for the Biot coefficient are obtained as

$$0.655 \leq \alpha \leq 0.665 \tag{23}$$

These values compare very favourably with the value of $\alpha \approx 0.70$ used in a previous investigation (Selvadurai and Najari [9]) of thermo-poroelastic phenomena associated with a fluid inclusion in the Cobourg Limestone using a typical value for limestone suggested by Wang [33]. Selvadurai and Nguyen [8] cite a value of $\alpha \approx 0.60$ for intact granite of the Canadian Shield, for which the porosity can be in the region of 0.3% and a permeability in the range 4.5×10^{-17} m^2.

6 Discussion

The partitioning of external stresses between the pore fluid and the porous skeleton of a geomaterial is a key concept in geomechanics applications. In poroelasticity, the parameters contributing to the partitioning process include the constitutive properties of all phases of the geomaterial. Alteration of the skeletal properties, including poroelastic damage [60] and failure of the skeleton [61,62], will be controlled by the partitioning process. Within the framework of Biot's [2] poroelasticity theory, the Biot parameter influences the partitioning process and depends on the compressibility characteristics of the fluid-free porous skeleton (K_D) and the compressibility of the solid material (K_S) comprising the porous skeleton. The procedure for estimating K_D is straightforward since pore fluids can be removed by conventional drying techniques. With ultra-low

permeability geomaterials [$K \in (10^{-23}, 10^{-20})$ m^2], unless the pore space is saturated in the in situ state of sample recovery, and maintained saturated, conventional techniques for measuring K_S have limitations. Testing is further complicated when the low permeability material has a dominant internal fabric requiring RVEs that can accommodate spatial heterogeneity. With some geomaterials, such as the Cobourg Limestone, the heterogeneity is visible, whereas with others, like Indiana limestone, the heterogeneity is not immediately evident but manifests in the assessment of hydraulic properties [63,64]. Cobourg Limestone presents a unique challenge requiring alternative procedures to estimate K_S; the individual volume fractions of the basic minerals and the respective volume fractions of the lighter and darker phases composing the fabric have to be determined. For Cobourg Limestone, XRT techniques to characterize the fabric have limitations due to the large test specimens, high overall density, absence of a density contrast between the lighter and darker phases and availability of a XRT scanner with sufficient penetrating power. Volume and area fractions therefore have to be based on dissection of representative specimens. The estimation of the effective solid bulk moduli requires the use of a composite materials approach, where the individual bulk moduli of the calcite, dolomite, quartz and clay phases are estimated. Determining these values from fundamental experiments requires discerning experimentation, and this research uses estimated values from published literature. There is wide variability in the values for the bulk moduli reported in the literature; the values chosen for the calculations are widely accepted results. The theoretical basis for estimating K_S relies on widely accepted developments in the theory of multi-phasic elastic materials. Further improvements to these estimates are possible, but in view of the estimations indicated previously, such refinements are perhaps unwarranted. Finally, the volume fractions for the geological species identified as the *lighter* and *darker* phases need to be determined accurately to estimate the Biot coefficient. Despite the wide range assigned for the parameter V_{DR}, its influence on the Biot coefficient is not large. This suggests that, despite the visual heterogeneous appearance and the variability in the volume fractions of *calcite*, *dolomite*, *quartz* and *clay* in the lighter and darker phases, the effective bulk compressibility of the solid material throughout the Cobourg Limestone is relatively constant.

7 Concluding remarks

Assessing the geomechanical properties of Cobourg Limestone is a challenge owing to its observable heterogeneity and extremely low permeability. The heterogeneity of the limestone requires relatively large samples (150 mm diameter) to account for the nodular fabric. This paper focuses on the estimation of the Biot coefficient, a key factor that controls the partitioning of applied stresses to the pore fluid and skeletal counterparts. The paper demonstrates that large specimen laboratory experiments are the most appropriate for accurately determining the skeletal bulk modulus of the Cobourg Limestone. The extremely low permeability of the Cobourg Limestone places a significant restriction on the use of the conventional full saturation procedure of a large sample and its subsequent pore fluid pressurization for estimating the compressibility of the solid phase constituting the porous fabric. A basic assessment of the volume fractions of the constituent minerals together with theoretical estimates for effective compressibility for a multi-phasic elastic material can be adopted to obtain the effective compressibility of the solid phase. This approach, combined with estimates for the compressibility of the minerals given in the literature, can be used to estimate the Biot coefficient for the heterogeneous, low permeability Cobourg Limestone. The approach can be further improved if XRT images of the lighter grey and darker regions of the limestone can be accurately produced. The paper relies on the theoretical concepts embodied in the *Voigt–Reuss–Hill* estimate and the *Hashin–Shtrikman* estimates to derive the Biot coefficient. Other theoretical approaches can be employed to estimate the compressibility of the solid material, but these require further theoretical and experimental research. Here, analytical approaches provide estimates of the solid phase compressibility of the heterogeneous limestone, giving a set of bounds for the Biot coefficient of the Cobourg Limestone that is consistent with the single value reported in the literature. The important contribution of the paper is the presentation of a general methodology that is suitable for estimating geomechanical properties of other complex geomaterials that are controlled by spatial heterogeneity at the sample scale and where saturation of the sample for the estimation of K_S is not feasible due to extremely low permeabilities.

Acknowledgements The work described in this paper was supported by a Discovery Research Grant awarded by the Natural Sciences and Engineering Research Council of Canada and research support from the Nuclear Waste Management Organization (NWMO) of Ontario, Canada. The author is grateful to Mr. Tom Lam and Mr. Mark Jenson of NWMO for their support and valuable suggestions. The author acknowledges the valuable assistance of past and current members of the Environmental Geomechanics

Group (A. P. Suvorov, M. Najari, P. A. Selvadurai, A. Glowacki, A. Letendre, B. Hekimi, L. Jenner, S. Rezaei Niya, J.-B. Regnet and J. Bartczak) in various aspects of the research. The very useful suggestions of the reviewers are gratefully acknowledged.

References

1. Selvadurai, A.P.S.: Geomechanical characterization of the Cobourg limestone. In: Nuclear Waste Management Organization Technical Report TR-2018 (2018)
2. Biot, M.A.: General theory of three-dimensional consolidation. J. Appl. Phys. **12**, 155–164 (1941)
3. Terzaghi, K.: Die Berechnung der Durchlassigkeitsziffer des Tones aus Dem Verlauf der Hydrodynamischen Spannungserscheinungen. Akad Wissensch Wien Sitzungsber Mathnaturwissensch Klasse IIa **142**, 125–138 (1923)
4. Coussy, O.: Poromechanics. Wiley, New York (2004)
5. Selvadurai, A.P.S.: The analytical method in geomechanics. Appl. Mech. Rev. **60**, 87–106 (2007)
6. Cheng, A.H.-D.: Poroelasticity. Springer, Berlin (2015)
7. Selvadurai, A.P.S., Suvorov, A.P.: Thermo-Poroelasticity and Geomechanics. Cambridge University Press, Cambridge (2016)
8. Selvadurai, A.P.S., Nguyen, T.S.: Computational modeling of isothermal consolidation of fractured porous media. Comput. Geotech. **17**, 39–73 (1995)
9. Selvadurai, A.P.S., Najari, M.: The thermos-hydro-mechanical behaviour of the argillaceous Cobourg Limestone. J. Geophys. Res. Solid Earth (2017). https://doi.org/10.1002/2016JB013744
10. Selvadurai, A.P.S., Suvorov, A.P., Selvadurai, A.P.: Thermo-hydro-mechanical processes in fractured rock formations during a glacial advance. Geosci. Model Dev. **8**, 2167–2185 (2015)
11. Cowin, S.C.: Bone Mechanics Handbook. Taylor and Francis, New York (2001)
12. Giorgio, I., Andreaus, U., Scerrato, D., dell'Isola, F.: A visco-poroelastic model of functional adaptation in bones reconstructed with bio-resorbable materials. Biomech. Model. Mechanobiol. **15**(5), 1325–1343 (2016)
13. Rosi, G., Placidi, L., dell'Isola, F.: "Fast" and "slow" pressure waves electrically induced by nonlinear coupling in Biot-type porous medium saturated by a nematic liquid crystal. Zeitschrift für angewandte Mathematik und Physik **68**(2), 51 (2017). https://doi.org/10.1007/s00033-017-0795-7
14. Pence, T.J.: On the formulation of boundary value problems with incompressible constituent constraints in finite deformation poroelasticity. Math. Model. Meth. Appl. Sci. **35**, 1756–1783 (2012)
15. Selvadurai, A.P.S., Suvorov, A.P.: Coupled hydro-mechanical effects in a poro-hyperelastic material. J. Mech. Phys. Solids **91**, 311–333 (2016)
16. Selvadurai, A.P.S., Suvorov, A.P.: On the inflation of poro-hyperelastic annuli. J. Mech. Phys. Solids **107**, 229–252 (2017)
17. Suvorov, A.P., Selvadurai, A.P.S.: On poro-hyperelastic shear. J. Mech. Phys. Solids **96**, 445–459 (2016)
18. Bruggeman, J.R., Zanger, C.N. and Brahtz, J.H.A.: Memorandum to Chief Designing Engineer: Notes on analytical soil mechanics, US Dept. of the Interior, Tech. Memorandum, No. 592 (1939)
19. Skempton, A.W.: The pore pressure coefficients A and B. Géotechnique **4**, 143–147 (1954)
20. Bishop, A.W.: Soils and soft rocks as engineering materials. Inaug. Lect. Imp. Coll. Sci. Tech. **6**, 289–313 (1966)
21. Selvadurai, A.P.S., Letendre, A., Hekimi, B.: Axial flow hydraulic pulse testing of an argillaceous limestone. Env. Earth Sci. **64**, 2047–2085 (2011)
22. Selvadurai, A.P.S., Jenner, L.: Radial flow permeability testing of an argillaceous limestone. Ground Water **51**, 100–107 (2013)
23. Selvadurai, A.P.S., Najari, M.: Isothermal permeability of the Argillaceous Cobourg Limestone. Oil and Gas Sci. Tech. (2016). https://doi.org/10.2516/ogst/2015039
24. Selvadurai, A.P.S., Glowacki, A.: Stress-induced permeability alterations in an argillaceous limestone. Rock Mech. Rock Eng **50**, 1079–1096 (2017)
25. Carmichael, R.S.: Practical Handbook of Physical Properties of Rocks and Minerals. CRC Press, Boca Raton (1990)
26. Berge, P.A., Berryman, J.G.: Realizability of negative pore compressibility in poroelastic composites. J. Appl. Mech **62**, 1053–1062 (1995)
27. Redfern, S.A.T., Angel, R.J.: High-pressure behaviour and equation of state of calcite, $CaCO_3$. Contrib. Mineral Petrol. **134**, 102–106 (1999)
28. Vanorio, T., Prasad, M., Nur, A.: Elastic properties of dry clay mineral aggregates, suspensions and sandstones. Geoph. J. Int. **155**, 319–326 (2003)
29. Lin, C.-C.: Elasticity of calcite: thermal evolution. Phys. Chem. Miner. **40**, 157–166 (2013)
30. Vilks, P., Miller, N.H.: Evaluation of Experimental Protocols for Characterizing Diffusion in Sedimentary Rocks, Nuclear Waste Management Division Report TR-2007-11, Toronto. Atomic Energy of Canada Limited, ON (2007)
31. Selvadurai, A.P.S., Najari, M.: Laboratory-scale hydraulic pulse testing: influence of air fraction in the fluid-filled cavity in the estimation of permeability. Geotechnique **65**, 124–134 (2015)
32. Detournay, E., Cheng, A.H.-D.: Comprehensive rock engineering: Principles, practice and projects. In: Hudson, J.A. (ed.) Fundamentals of Poroelasticity, vol. 1, pp. 113–171. Pergamon Press, Oxford (1993)
33. Wang, H.F.: Theory of Linear Poroelasticity with Applications to Geomechanics and Hydrogeology. Princeton University Press, Princeton (2000)
34. Lion, M., Skoczylas, F., Ledésert, B.: Determination of the main hydraulic and poro-elastic properties of a limestone from Bourgogne, France. Int. J. Rock Mech. Min. Sci. **41**, 915–925 (2004)
35. Wang, Y., Agostini, F., Skoczylas, F., Jeannin, L., Portier, É.: Experimental study of the gas permeability and bulk modulus of tight sandstone and changes to its pore structure. Int. J. Rock. Mech. Min. Sci. **91**, 203–209 (2017)
36. Armand, G., Conil, N., Talandier, J., Seyedi, D.M.: Fundamental aspects of the hydromechanical behaviour of the Callovo–Oxfordian claystone: from experimental studies to model calibration and validation. Comp. Geotech. **85**, 277–286 (2017)

37. Selvadurai, A.P.S., Carnaffan, P.: A transient pressure pulse method for the measurement of permeability of a cement grout, Can. J. Civil Eng. **24**, 489–502 (1997)
38. Selvadurai, A.P.S.: Partial Differential Equations in Mechanics, Vol. 1. Fundamentals, Laplace's Equation, the Diffusion Equation, the Wave Equation. Springer, Berlin (2000)
39. Carslaw, H.S., Jaeger, J.C.: Conduction of Heat in Solids. Oxford Science Publications, Oxford (1959)
40. Selvadurai, A.P.S.: Influence of residual hydraulic gradients on decay curves for one-dimensional hydraulic pulse tests. Geophys. J. Int. **177**, 1357–1365 (2009)
41. Voigt, W.: Lehrbuch der Kristallphysik. Teubner, Leipzig, B.G (1928)
42. Reuss, A.: Berechnung der Fließgrenze von Mischkristallen auf Grund der Plastizitätsbedingung für Einkristalle. J. Appl. Math. Mech **9**, 49–58 (1929)
43. Hill, R.: The elastic behaviour of a crystalline aggregate. Proc. Phys. Soc. **65**, 349–354 (1952)
44. Hill, R.: Self-consistent mechanics of composite materials. J. Mech. Phys. Solids **13**, 213–222 (1965)
45. Hashin, Z., Shtrikman, S.: A variational approach to the elastic behavior of multiphase minerals. J. Mech. Phys. Solids **11**, 127–140 (1963)
46. Hashin, Z.: The elastic moduli of heterogeneous materials. J. Appl. Mech. **29**, 143–150 (1962)
47. Walpole, L.J.: On bounds for the overall elastic moduli of inhomogeneous Systems. J. Mech. Phys. Solids **14**, 151–62 (1966)
48. Hale, D.K.: The mechanical properties of composite materials. J. Mat. Sci. **11**, 2105–2141 (1976)
49. Christensen, R.M.: Mechanics of Composite Materials. Wiley, New York (1979)
50. Francfort, G.A., Murat, F.: Homogenization and optimal bounds in linear elasticity. Arch. Rat. Mech. Anal. **94**, 307–334 (1986)
51. Sisodia, P., Verma, M.P.: Polycrystalline elastic moduli of some hexagonal and tetragonal materials. Phys. Stat. Sol. **122**, 525–534 (1990)
52. Ju, J.W., Chen, T.M.: Micromechanics and effective moduli of elastic composites containing randomly dispersed ellipsoidal inhomogeneities. Acta Mech. **103**, 103–121 (1994a)
53. Ju, J.W., Chen, T.M.: Effective elastic moduli of two-phase composites containing randomly dispersed spherical inhomogeneities. Acta Mech. **103**, 123–144 (1994b)
54. Nemat-Nasser, S., Hori, M.: Micromechanics: Overall Properties of Heterogeneous Materials, 2nd Ed., North-Holland (1999)
55. Torquato, S., Yeong, C.L.Y., Rintoul, M.D., Milius, D.L., Aksay, I.A.: Elastic properties and structure of interpenetrating Boron Carbide/Aluminum multiphase composites. J. Am. Ceram. Soc. **82**, 1263–1268 (1999)
56. Lin, P.J., Ju, J.W.: Effective elastic moduli of three-phase composites with randomly located and interacting spherical particles of distinct properties. Acta Mech. **208**, 11–26 (2009)
57. Suvorov, A.P., Selvadurai, A.P.S.: Macroscopic constitutive equations of thermo-poroviscoelasticity derived using eigenstrains. J. Mech. Phys. Solids **58**, 1461–1473 (2010)
58. Avseth, P., Mukerji, T., Mavko, G.: Quantitative Seismic Interpretation: Applying Rock Physics Tools to Reduce Interpretation Risk. Cambridge University Press, Cambridge (2005)
59. Mavko, G., Mukerji, T.: Dvorkin: The Rock Physics Handbook. Tools for Seismic Analysis of Porous Media. Cambridge University Press, Cambridge (2009)
60. Selvadurai, A.P.S.: Stationary damage modelling of poroelastic contact. Int. J. Solids. Struct. **41**, 2043–2064 (2004)
61. Selvadurai, A.P.S., Suvorov, A.P.: Boundary heating of poroelastic and poro-elastoplastic spheres. Proc. R. Soc. A: Math., Phys. Engng Sci. **468**(2145), 2779–2806 (2012)
62. Selvadurai, A.P.S., Suvorov, A.P.: Thermo-poromechanics of a fluid-filled cavity in a fluid-saturated geomaterial. Proc. R. Soc. A: Math. Phys., Engng Sci **470**(2163), 20130634 (2014)
63. Selvadurai, A.P.S., Selvadurai, P.A.: Surface permeability tests: experiments and modelling for estimating effective permeability. Proc. R. Soc. A: Math. Phys., Engng Sci. **466**(2122), 2819–2846 (2010)
64. Selvadurai, P.A., Selvadurai, A.P.S.: On the effective permeability of a heterogeneous porous medium: the role of the geometric mean. Phil. Mag. **94**, 2318–2338 (2014)